

## JOSEPHSON JUNCTION NETWORK AS A TOOL TO SIMULATE INTERGRAIN SUPERCONDUCTING CHANNELS IN YBCO FILMS

G. ROTOLI\* AND C. DE LEO

*Università dell'Aquila, (\*) INFN – U.d.R. L'Aquila,  
Località Monteluco, Roio Poggio, I67040 L'Aquila, Italy  
E-mail: rotoli@ing.univaq.it*

G. GHIGO AND L. GOZZELINO

*INFN - U.d.R. Torino-Politecnico; INFN - Sez. Torino  
Politecnico di Torino, c.so Duca degli Abruzzi 24, 10129 Torino, Italy  
E-mail: ghigo@polito.it*

C. CAMERLINGO

*Istituto di Cibernetica del Consiglio Nazionale delle Ricerche  
Via Toiano 6, 80072 Arco Felice, Italy  
E-mail: carlo@fiscc.cib.na.cnr.it*

Recent considerations on the physics of  $\text{YBa}_2\text{Cu}_3\text{O}_{7-\delta}$  films made possible explaining their transport properties as flow of supercurrents through links between the granular structure of the film. The present work deals with the analysis of the Josephson junction network as a discrete set of parallel junctions (1D array) in quasi-static conditions and is aimed to compare the results of the simulations with the experimental findings, in particular with the plateau-like features in the critical current dependence on the magnetic field. Different regimes and vortex phases have been individuated and discussed.

### 1 Introduction

One-dimensional arrays were suggested very early as building blocks for high  $T_c$  superconductors (HTS) [1]. Nevertheless the matter was limited to phenomenological considerations due to the complex nature of phenomena occurring in HTS bulk materials. Only recently some particular characteristics of HTS  $\text{YBa}_2\text{Cu}_3\text{O}_{7-\delta}$  films gave hints toward the modeling the film transport properties as flow of supercurrents through links between granular structures [2,3]. In this paper we report on computer simulation analysis of the Josephson junction (JJ) network as a discrete set of parallel junctions (1D array), in quasi-static conditions. The coupling between the junctions of the array is introduced via standard fluxoid quantization rule and self-inductance of superconducting path between junctions of the network. In this model the coupling is represented by a suitable value of the parameter:

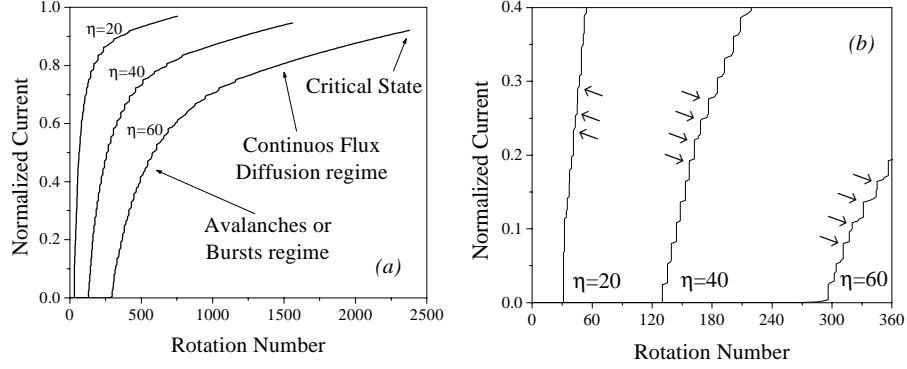


**Figure 1.** (a) Normalized current as function of Rotation Number, i.e. the number of flux quanta entering the array, for three values of active-end normalized magnetic field. In this case the parameters of the array are the following:  $\beta_L = 225$ ,  $N = 40$ ,  $\alpha = 1$ . (b) Magnification of the low-current region of Fig.1 (a), showing the dynamical mechanism of penetration of the field in the array. Arrows indicate approximately the start of a series of sharp increases in rotation number. This mechanism is referred as "avalanches or burst regime"

$$\beta = \frac{2\pi I_0(0)L}{\Phi_0}$$

where  $I_0(0)$  is the zero field Josephson supercurrent and  $L$  is the superconducting path inductance. Single junctions of the network are modeled as RSJ elements (at this moment all perfectly equal without spread in the critical currents or electrical parameters with an intermediate damping corresponding to  $\beta_C$ ). Equations describing the array can be written as DSG (Discrete Sine-Gordon) equation in the following form [4,5]:

$$\vec{\varphi}_{tt} + \alpha \vec{\varphi}_t + \sin \vec{\varphi} = \mathbf{M} \vec{\varphi} + \Gamma \vec{f} + \vec{\gamma}$$

where  $\vec{\varphi}$  is the phase vector representing the phase in each junction (here the subscripts denote first and second derivatives in  $t$ ),  $\vec{f}$  is the frustration vector,  $\mathbf{\Gamma}$  is the matrix relating frustration to phases,  $\mathbf{M}$  is the coupling matrix which is proportional to  $1/\beta_L$  and contains in general both self-inductance and mutual inductance terms (here we consider only next neighbor mutual inductance),  $\alpha = (1/\beta_C)^{1/2}$  is the damping parameter, finally  $\vec{\gamma}$  is the induced bias current vector (in this model representing the AC magnetization current generated in the sample in the experiment reported below). In order to reproduce the transport current mechanism

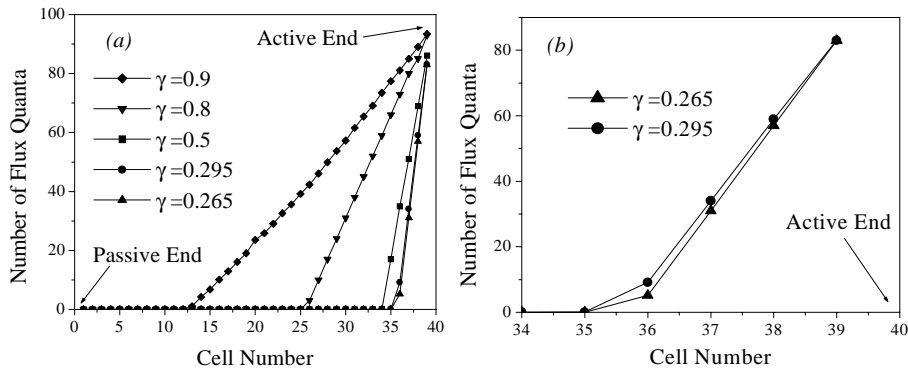


**Figure 2.** (a) Normalized magnetic flux distribution  $h=\Delta\phi/2\pi$ , i.e. the number of flux quanta for each cell in the array, for different values of current. (b) Magnetic flux distribution plotted just before and after the process of penetration of an avalanche of flux quanta in the array in the "avalanche regime". A burst occurring between the two current values distributes about 10 fluxons in the holes near the active end. The parameters of the array are:  $\beta_L=225$ ,  $N=40$ ,  $\alpha=1$ , the normalized magnetic field is  $\eta=40$ .

used in the experiments, the magnetic field was introduced only at one extreme (active end) of the array. The active end represents the physical edge in which the field penetrates in the film. Magnetic field (here measured in terms of number of flux quanta) progressively advances toward the full penetration at the center of the sample, represented by the other extreme of the array (passive end).

## 2 Results and discussion

An illustration of the dynamics of JJ array is shown in Fig.1a, where we report the normalized current as function of the Rotation Number (the number of flux quanta entering the array), for three values of the normalized magnetic field at the active end, as shown in the legend. The critical state is reached at the end of each curve. The parameters of the array are the following:  $\beta_L = 225$ ,  $N = 40$ ,  $\alpha = 1$ . In a typical simulation the current bias current is increased starting from zero in a given magnetic field, until the array becomes critical and a finite voltage appears at its ends. Before critical current is reached, several avalanches of Josephson vortices (corresponding in this model to a  $2\pi$  wrap in the phases) penetrate in the array from the active end. This process stresses out the strongly discrete nature of system. It continues until the array is unable to accommodate other flux quanta. At this values of bias current the critical state sets on. For lower current values, flux quanta avalanches dominate the dynamical mechanism of penetration of the field in the array, as shown in the Fig.1b. The arrows indicate approximately the start of a

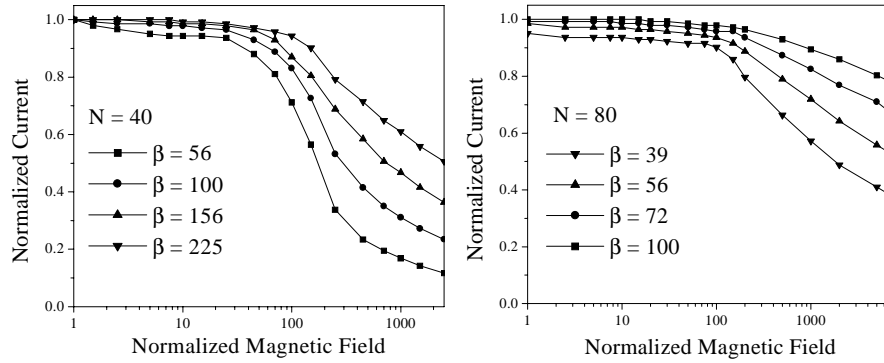


**Figure 3.** Magnetic field pattern for an array of  $N=40$  Josephson junctions (a) and for an array of  $N=80$  Josephson junctions (b).

series of sharp increases in rotation number. We refer to this mechanism as "avalanches or burst regime". For higher (subcritical) current values, avalanches become less evident because the array almost continuously is penetrated by a large number of flux quanta. We refer to this regime as the "continuous flux diffusion regime" (cf. Fig.1a).

In Fig.2 the normalized magnetic flux distribution  $h=\Delta\phi/2\pi$ , evaluated as phase difference  $\Delta\phi=\phi_{k+1}-\phi_k$ , over the array (the number of flux quanta for each cell in the array) is shown. In particular in Fig.2a the number of flux quanta in each cell is plotted for different values of current at a given value of external normalized magnetic field. Higher currents correspond to complete penetration of flux in the array, whereas for lower currents the flux is essentially concentrated near the active end. The flux distribution is essentially linear, as in the Bean model, and also for higher subcritical currents it is clear that the passive end is again untouched by flux penetration occurring also at few cells of distance, thus confirming that criticality is connected to full penetration. In Fig.2b the magnetic flux distribution is plotted just before and after the process of penetration of an avalanche of flux quanta in the array in the "avalanche regime". It can be view how flux quanta will distribute along the first cells near the active end.

In Fig.3a we show the magnetic field pattern for a small array of  $N=40$  JJ. The plateau extends over some decades. The values of  $\beta_L$  can be as high as 225 to obtain the largest plateau. In Fig.3b the same plateau is shown for an array of  $N=80$  JJ. The plateau extends approximately over the same length of the previous case, but the values of  $\beta_L$  are relatively smaller, ranging from 39 to 100. It results that the plateau length depends on the coupling  $\beta_L$  between the JJ and on the number of JJ

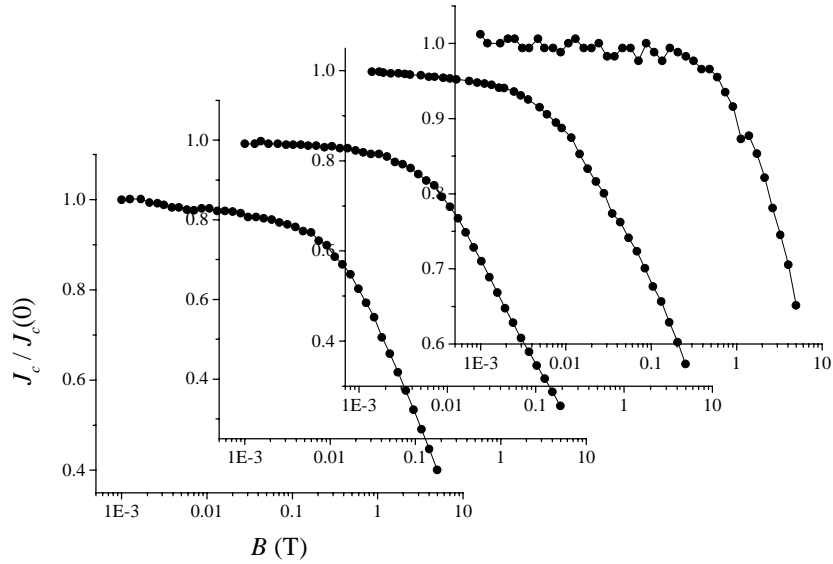


**Figure 4.** Typical experimental curves for the field-dependence of the critical current density (different  $\text{YBa}_2\text{Cu}_3\text{O}_{7-\delta}$  films at  $T = 36$  K).

in the array. It is found that the normalized crossover field  $b^*$  (defined as the normalized field where  $J_c$  reaches a given fraction of the zero-field value [2]) depends roughly on  $N\beta_L^{1/2}$  in all simulations. It means that also for small values of  $\beta_L$  (typically between 1 and 10) it should be possible to have *large* value of  $b^*$  if the number of junctions is high (however for such small  $\beta_L$  effects of mutual inductance cannot be typically ignored and a full inductance model have to be considered). In all simulations  $\alpha=1$ .

The experimental dependence of the critical current density on the applied magnetic field in YBCO thin films has been obtained from susceptibility measurements [2]. As a qualitative comparison we plot in Fig.4 typical results for different samples at  $T = 36$  K. The characteristic feature is the plateau in the  $J_c$  vs.  $\log B$  curves, that can be explained in terms of Josephson currents through the nanosized granular structure of the film [2]. It has been shown that such links have a statistical length distribution, with a mean value of the order of 20 nm [6].

### 3 Conclusions

We analyzed the Josephson junction network as a discrete set of parallel junctions in

quasi-static conditions and we made a comparison between the results of the simulations and the experimental findings, in particular the plateau features in the critical current dependence on the magnetic field. Though the comparison is at a qualitative level, the correspondence of the results is quite encouraging, if we take into account that the simulations do not consider the finite length of the junctions as well as the length distribution. All the experimental findings are then expected to be accounted for by more detailed future analysis that must be aimed to consider these aspects. The main feature of the simulations consists in the capability to reproduce the large  $J_c$  vs.  $B$  plateau and to establish that its shape depends on the coupling between junctions. It must be emphasized that this kind of simulation is very promising because it allows to have  $J_c$  vs.  $B$  curves, normalized  $V$  vs.  $I$  characteristics and spatial flux distribution in the same analysis framework.

#### 4 Acknowledgment

The authors wish to thank E. Mezzetti for helpful discussions. This work was supported on MURST COFIN98 Project "Dynamics and Thermodynamics of vortex structures in superconductive tunneling".

#### References

1. F. Parodi and R. Vaccarone, *Physica C*173, 56-64, 1991.
2. E. Mezzetti, R. Gerbaldo, G. Ghigo, L. Gozzelino, B. Minetti, C. Camerlingo, A. Monaco, G. Cuttone, A. Rovelli, *Phys. Rev. B*60, 7623, 1999.
3. J. Jung, H. Darhmaoul, H. Yan, *Supercond. Sci. Technol.* 11, 973, 1998.
4. C. Lucheroni, *Phys. Rev. B*55, 6559, 1997.
5. G. Filatrella, A. Petraglia and G. Rotoli, *Eur. J. Phys.* 12, 23-30, 1999.
6. E. Mezzetti, A. Chiodoni, R. Gerbaldo, G. Ghigo, L. Gozzelino, B. Minetti, C. Camerlingo and A. Monaco, *Physica C*332, 126, 2000.